Synchrotron Radiation Solution X-ray Scattering Study of the pH Dependence of the Quaternary Structure of Yeast Pyruvate Decarboxylase

Stephan König,*,‡ Dmitri Svergun,§,∥ Michel H. J. Koch,§ Gerhard Hübner,‡ and Alfred Schellenberger‡

Institute of Biochemistry, Department of Enzymology, Martin-Luther-Universität Halle-Wittenberg, Weinbergweg 16a, D-4050 Halle/S, Federal Republic of Germany, and European Molecular Biology Laboratory, Hamburg Outstation, EMBL c/o DESY, Notkestrasse 85, D-2000 Hamburg 52, Federal Republic of Germany

Received December 24, 1991; Revised Manuscript Received June 24, 1992

ABSTRACT: The pH dependence of the quaternary structure of pyruvate decarboxylase from yeast was studied in the range $6.2 < pH < 8.4$. There is an equilibrium with a midpoint around pH 7.5 between tetramers and dimers, and the catalytic activity of the enzyme depends on the volume fraction of tetramer. This equilibrium may provide an additional regulating mechanism besides substrate activation since accumulation of pyruvate would lead to a reduction in pH and hence an increase of the concentration of the catalytically active tetramer. Radiation damage during the X-ray scattering experiments results in a shift of this equilibrium and in the formation of octamers. These effects could be circumvented and analyzed using experimental and data processing methods which can be readily applied to other radiation-sensitive systems. The low-resolution shapes of the dimers and tetramers were determined from the scattering curves using spherical harmonics. The results indicate that a conformational change must occur in the dimers upon formation of the tetramers, in agreement with earlier circular dichroism measurements.

PDC[1] is a key enzyme in alcoholic fermentation. It exists in yeast (Holzer et al., 1956), some bacteria (Bringer-Meyer et al., 1986; Neale et al., 1987), and plant seeds (Oba & Uritani, 1975; Zehender et al., 1987; Leblova & Valik, 1981; Leblova & Martinec, 1987; Leblova et al., 1989; Lee & Langston-Unkefer, 1985) and has been isolated from a large number of organisms. It catalyzes the nonoxidative decarboxylation of 2-oxo acids to the corresponding aldehydes according to the reaction

$$R\text{–}CO\text{–}COO^- + H_2O \rightarrow R\text{–}CHO + OH^- + CO_2$$

The enzyme is a thiamin diphosphate dependent lyase. It binds its cofactors thiamin diphosphate (TDP) and Mg^{2+} ions in a quasi-irreversible manner at pH 6 (Schellenberger & Hübner, 1967), in contrast with all other enzymes in this class where this binding is reversible.

Above pH 7 the cofactors are released and catalytically inactive apoenzyme is obtained which, in the presence of appropriate concentrations of cofactors, can be readily reassembled to the active holoenzyme at pH values below 7 (Schellenberger & Hübner, 1967). Gounaris et al. (1975) first observed that after gel filtration above pH 8 the enzyme only has half (118 000) of its original molecular weight (230 000). These observations were confirmed in a previous X-ray solution scattering study on PDC from brewers' yeast (Hübner et al., 1990), and it was shown that the kinetics of dissociation at pH 8.0 and inactivation caused by the release of the cofactors were identical.

Whereas the catalytic and assembly processes in PDC from brewers' yeast were investigated in detail in the past (Jordan et al., 1979; Schellenberger, 1982; Koike & Koike, 1982; Zeng, 1991), relatively little is known about the three-dimensional structure of the enzyme. This is explained by the fact that nearly 80 years passed between the first purification of PDC from brewers' yeast (Neuberg & Karczag, 1911) and the obtainment of crystals adequate for X-ray diffraction studies (Dyda et al., 1990).

The following is known about the quaternary structure: Several studies have shown that PDC is a tetramer (Ullrich et al., 1966; Ullrich & Kempfle, 1969; Hübner et al., 1975). Depending on the species from which the enzyme was purified, PDC has been described as a homotetramer (α_4) consisting of only one type of subunit with molecular weights between 60 000 and 65 000 (Bringer-Meyer et al., 1986; Oba & Uritani, 1975; Zehender et al., 1987; Kuo et al., 1986) or as an $\alpha_2\beta_2$ tetramer with two types of subunits having different molecular weights. PDC from brewers' yeast has an $\alpha_2\beta_2$ structure. The two types of subunits have different molecular weights (α = 59 000; β = 61 000) (Sieber et al., 1983) and also differ in amino acid composition and sequence (Zehender & Ullrich, 1985; Zehender et al., 1987). Whereas the gene sequence of PDC from haploid yeast is known (Hohmann & Cederberg, 1990), the sequence determination of the gene(s) for PDC from brewers' yeast is still in progress (Hohmann, private communication). Besides the structures described above, isozymes with significantly higher molecular weights (120 000 and 370 000) were also described (Zehender et al., 1987). Our observations have shown that the subunit ratio α:β is not always 1:1 in freshly prepared PDC but can reach values up to 2:1. This points to a more complex structure of PDC in solution than hitherto accepted. The present paper is a contribution to the clarification of this problem.

Solution scattering studies on PDC from brewers' yeast were performed nearly 20 years ago by Pilz (1973), who calculated a model based on a rotational ellipsoid. This model was later refined by Müller et al. (1979) using two three-axial ellipsoids twisted perpendicularly to their short axis. Synchrotron radiation solution scattering experiments were also done (Hübner et al., 1990), and the pH-dependent dissociation

‡ Martin-Luther-Universität.
§ European Molecular Biology Laboratory.
∥ On leave from the Institute of Crystallography, Academy of Sciences of Russia, Leninsky pr. 59, Moscow 117333, Russia.

[1] Abbreviations: ADH, alcohol dehydrogenase; Hepes, *N*-(2-hydroxyethyl)piperazine-*N*′-2-ethanesulfonic acid; MES, 4-morpholineethanesulfonic acid; PDC, pyruvate decarboxylase; TDP, thiamin diphosphate; Tricine, *N*-[tris(hydroxymethyl)methyl]glycine.

0006-2960/92/0431-8726$03.00/0

of PDC was directly proven. The experiments below investigate the three-dimensional structure of PDC in solution in the pH range from 6.2 to 8.4.

EXPERIMENTAL PROCEDURES

Preparation of PDC and Kinetic Measurements. PDC was isolated from fresh or dried brewers' yeast (Export brewery Wernesgrün) (Ullrich et al., 1966; Sieber et al., 1983). SDS–polyacrylamide gel electrophoresis (Sieber et al., 1983) reveals only the bands due to the two subunits. The activity was monitored spectroscopically using the ADH (Serva)/NADH (Serva) system (Holzer et al., 1956). The concentrations of PDC were measured spectrophotometrically at 280 nm (ϵ = 281 000 M^{-1} cm^{-1}). Kinetic measurements were performed at 30 °C and 340 nm (ϵ = 6150 M^{-1} cm^{-1}) on different spectrometers [M40 (Carl Zeiss Jena), DU70 (Beckman), and Uvikon 940 (Kontron)]. MES, Hepes, and Tricine (Serva) were used as incubation buffers between pH 5 and 8.5. The specific activities after purification were between 50 and 60 units/mg (1 unit = 1 μM NADH turnover/min). PDC was stored at −15 °C in 3 M ammonium sulfate.

To determine the inactivation rate, the samples were incubated at 30 °C in Hepes buffer between pH 6.5 and 7.5 and in Tricine buffer between pH 7.5 and 8.5. Aliquots were taken at different times, and their catalytic activity was assayed as described above. The pseudo-first-order rate constant of inactivation was determined from the semilogarithmic plot of activity vs incubation time.

X-ray Solution Scattering. PDC in ammonium sulfate solution (minimum 10 mg) was centrifuged and redissolved in a minimum volume elution buffer [10 mM $(NH_4)_2SO_4$, pH 6.2)], desalted, and concentrated (up to 30 mg/mL) using a PD10 column (Pharmacia Biosystems). The X-ray scattering measurements were performed in the concentration range 2–7 mg/mL. The protein and ammonium sulfate concentrations had been optimized in preliminary experiments (Hübner et al., 1990).

The pH values were adjusted using 50 mM sodium glycine/phosphate buffer, pH 8.5, and incubated at 5 °C for at least 60 min to obtain equilibrium between the different oligomers. The specific activity, pH values, and protein concentrations were measured before and after the X-ray measurements. Only catalytically active samples with appropriate values were used further.

The solution scattering measurements were performed at 7 °C on the X33 camera (Koch & Bordas, 1983) of the EMBL in HASYLAB at the storage ring DORIS of the Deutsches Elektronen Synchrotron (DESY) at Hamburg using the standard data acquisition and evaluation systems (Boulin et al., 1986, 1988).

On the basis of previous experiments it was assumed that equilibrium between oligomers was reached after 1 h of incubation. To monitor any changes due to, for instance, radiation damage or beam movement, the X-ray scattering patterns in the range $0.094 < s < 1.382$ nm^{-1} were collected for solutions and corresponding buffers at intervals of 1 min for up to 10 min. The scattering vector $s = 4\pi \sin\theta/\lambda$ corresponds to the scattering angle 2θ and the wavelength λ (0.15 nm). Data reduction, background subtraction, and correction for the detector response and sample transmission were done using the program SAPOKO (Svergun & Koch, unpublished data) following standard procedures [see, e.g., Koch (1991)]. Distance distribution and size distribution functions were evaluated using the indirect transform method based on the regularization technique as implemented in the program GNOM (Svergun et al., 1988; Svergun, 1991). Shape determination

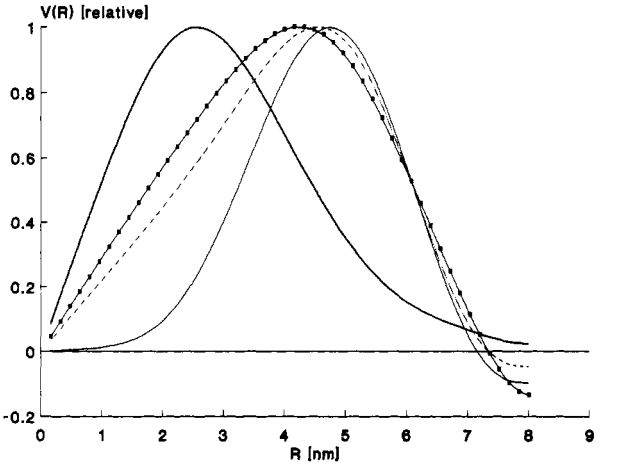

FIGURE 1: Volume distribution functions obtained in the hard spheres approximation: pH 6.2 (—); pH 7.1 (– –); pH 8.1 (–■–); pH 8.4 (—).

was performed using multipole expansion methods (Stuhrmann, 1970a,b; Svergun & Stuhrmann, 1991).

The data in the range $0.094 < s < 0.19$ nm^{-1} were not included in the fits since systematic errors (e.g., due to background variations resulting from small beam shifts) cannot be excluded. They were, however, used to check the validity of the analysis of the oligomer content.

RESULTS

The scattering patterns indicate that the PDC solutions are polydisperse, as already observed by Pilz (1973), but their detailed analysis as a function of exposure time indicates that the formation of oligomers larger than tetramers is due to the onset of radiation damage. To avoid the influence of radiation damage, only scattering patterns corresponding to the first minute of irradiation were used further.

The following approach was taken to analyze the data. In a first step the data were treated as a polydisperse system of spherical particles to obtain an estimate of the heterogeneity. The scattering from a polydisperse system of spheres is given by (Feigin & Svergun, 1987)

$$I(s) = \int_0^\infty i_0(sR)V^2(R)D_N(R)\,dR$$

where $i_0(sR)$ is the form factor of a sphere of radius R, $V(R)$ its volume, and $D_N(R)$ the size distribution function of the spheres. The volume distribution functions $D_V(R) = D_N(R)V(R)$ at different pH values are shown in Figure 1. At the limits of the pH range these curves correspond to monodisperse systems with an average particle radius around 2.5 nm at pH 8.4 and around 4.5 nm at pH 6.2. The result is unequivocal since deviations from sphericity of the particles in solution could only lead to a broadening of the $D_V(R)$ curves. The Porod volumes for pH 8.4 and 6.2 were estimated to be approximately 210 and 400 nm^3, respectively. Since the volume of a subunit (MW = 65 000) can be estimated to be around 80 nm^3, these results suggest that at pH 8.4 the solutions contain predominantly dimers, whereas at pH 6.2 tetramers are dominant. At intermediate pH values the samples seem to contain mixtures of these two types of particles.

To get information about the structure of the dimers and tetramers, the scattering data at pH 8.4 and 6.2, illustrated in Figure 2, were treated by assuming monodispersity. For a monodisperse system

$$I(s) = \int_0^{D_{max}} p(r)\frac{\sin sr}{sr}\,dr$$

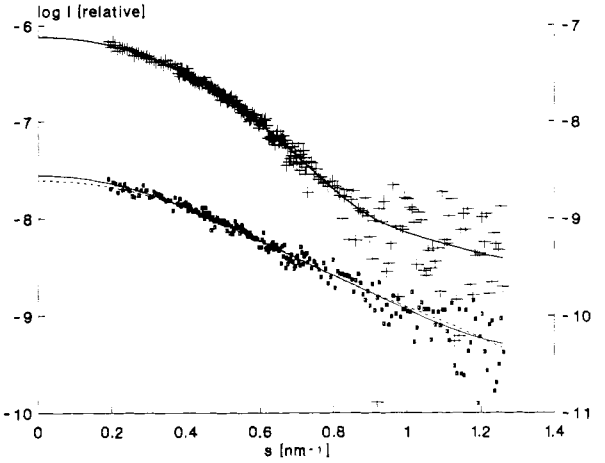

FIGURE 2: Scattering from dimer (pH 8.4) and tetramer (pH 6.2), respectively: experimental data (■ and +) and fitted curves (– –) and (—); scattering calculated from the lower resolution (L = 2) dimer model (—). The curves obtained from the higher resolution models of dimer and tetramer do not differ from the corresponding fitted curves (– – and —, respectively).

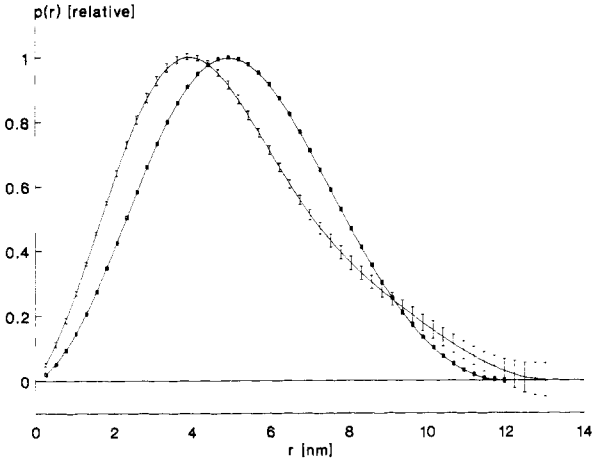

FIGURE 3: Distance distribution functions, $p(r)$, of the dimer (—) and tetramer (–■–). The propagated errors are shown only for the $p(r)$ of the dimer.

where $p(r)$ is the distance distribution function of the particles and D_{max} their maximum diameter (Feigin & Svergun, 1987). The distance distribution functions $p(r)$ were evaluated using the indirect transform technique. To estimate the maximum distances D_{max}, a series of calculations with varying D_{max} were performed for both curves. The resulting $p(r)$ functions are shown in Figure 3, and the fit between the corresponding scattering curves and the experimental data is illustrated in Figure 2. Note that the maximum dimension in the dimer is not smaller than that in the tetramer. The radius of gyration of the tetramer is 4.02 ± 0.03 nm and that of the dimer 3.86 ± 0.05 nm.

The shape of oligomers was estimated from the fitted scattering curves using spherical harmonics. The structure of a homogeneous particle $\rho(\mathbf{r})$ can be described by the angular shape function $F(\omega)$ defined as

$$\rho(\mathbf{r}) = 1, \quad 0 \le r < F(\omega) \qquad (1)$$

$$\rho(\mathbf{r}) = 0, \quad r \ge F(\omega)$$

This function can be expanded into the series

$$F(\omega) = \sum_{l=0}^{L} \sum_{m=-l}^{l} f_{lm} Y_{lm}(\omega) \qquad (2)$$

where $(r,\omega) = (r, \theta, \phi)$ are spherical coordinates, f_{lm} complex multipole coefficients, and $Y_{lm}(\omega)$ spherical harmonics (Stuhrmann, 1970a,b). The multipole coefficients are related by a system of nonlinear equations to the coefficients of the power series describing the scattering curve. Svergun and Stuhrmann (1991) developed a method to evaluate these coefficients by minimizing the discrepancy R_I between the experimental $I_{exp}(s)$ and model $I_{mod}(s)$ scattering intensities

$$R_I = \int_{s_{min}}^{s_{max}} |I_{exp}(s) - I_{mod}(s)| s^2 ds / \int_{s_{min}}^{s_{max}} I_{exp}(s) s^2 ds \qquad (3)$$

The resolution with which the shape can be restored is determined by the maximum order L of the spherical harmonic taken into consideration in eq 1. This number, in turn, depends on the relation between the particle size and the available range of the scattering curve. The maximum order of harmonic L can be estimated as $(s_{max}R_0 - 1)$, where R_0 is the radius of the equivalent sphere $[R_0 = (3V/4\pi)^{0.333}]$ (Svergun & Stuhrmann, 1991). Since identical parts of the scattering curves are considered for shape fitting, a better resolution is achieved for the tetramer. Indeed, for the dimer curve $s_{max}R_0 = 4.7$ and L = 2–3, whereas for the tetramer $s_{max}R_0 = 6.0$ and L = 4–5.

The results of the shape restoration (L = 2 for dimer and L = 4 for tetramer) are presented in Figure 4. In both cases three-axial ellipsoids evaluated from the invariants (radius of gyration, volume, maximum distance) were used as an initial approximation.

The use of harmonics up to L = 4 involves, in principle, 25 parameters, but these are not independent. Three parameters defining the particle orientation can be fixed. The fact that the small-angle scattering invariants (radius of gyration, volume, surface, average length) are combinations of the parameters imposes further restrictions on their independence. In the case of the tetramer the overwhelming dominance of the even harmonics (see Discussion) allows one to neglect the contributions from odd harmonics. In this case there are effectively not more than eight independent parameters, the use of which is fully justified by the range of scattering vectors and the quality of the processed data. The situation is less favorable in the case of the dimer, and the fit to the data of the low-resolution model (R_I = 3.5%) is worse than that of the tetramer (R_I = 0.44%), as illustrated in Figure 2. In particular, the maximum dimension of the model of the dimer is 11.1 nm, as opposed to the experimental value of 13 nm. Given the resolution of L = 2 (only three independent parameters), no better agreement can be achieved. The higher resolution model, shown in Figure 4, fits the scattering data in Figure 2 perfectly (R_I = 0.20%) and also displays two distinct subunits, but the use of eight independent parameters is not entirely justified as discussed below.

The consistency of the dimer and tetramer models allows one to go one step further in the analysis of the oligomer distribution and its dependence on pH and radiation damage. The estimates of the fractions of oligomers below are independent of whether the curves corresponding to higher or lower resolution models of the dimer are used since the differences between them are negligible compared to the experimental uncertainties.

The scattering from a system consisting of N oligomers can be expressed as a sum

$$I(s) = \sum_{j=1}^{N} \nu_j I_j(s) \qquad (4)$$

where ν_j and $I_j(s)$ denote the volume fraction and the scattering intensity of jth oligomer, respectively. For a given intensity

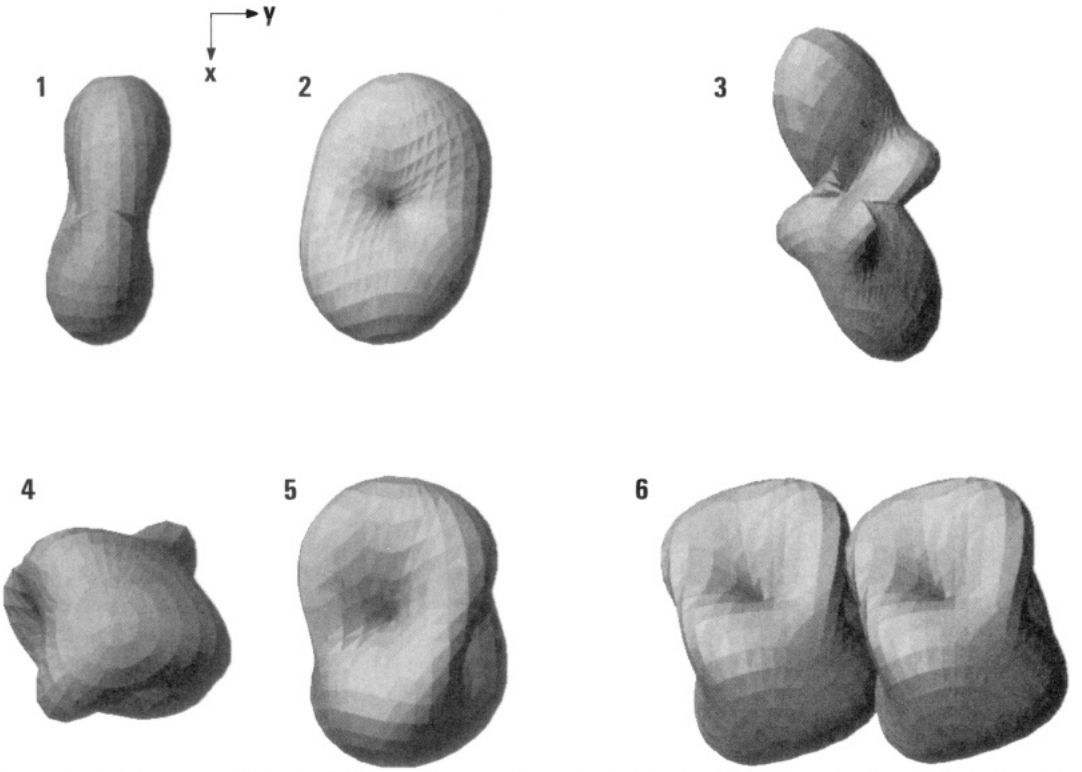

FIGURE 4: Shapes of the oligomers of PDC. (1) Dimer with a resolution of $L = 2$; (2) model 1 rotated 90° around the X axis; (3) dimer with $L = 4$; (4) tetramer at $L = 4$; (5) model 4 rotated 90° around the Y axis; (6) octamer consisting of two tetramers. The sizes of the (X,Y) square correspond to a length of 2 nm.

$I(s)$ and given set of basic curves $I_j(s)$, the relative amounts of the oligomers can be readily determined by a least-squares procedure minimizing the functional

$$\chi^2 = \sum_{k=1}^{K}\{[I(s_k) - \sum_{j=1}^{N} \nu_j I_j(s_k)]/\sigma_k\}^2 \qquad (5)$$

(here K is the number of experimental points and σ_k the standard deviation of the kth experimental point). The goodness-of-fit is expressed in terms of the χ^2 distribution as GoF = $P_\chi(\chi^2, K–N)$ (Bevington, 1969).

The curves for dimers and tetramers were used as basic functions in the series in eq 4, but since the experimental R_g values are in some cases as high as 5 nm, especially after several minutes of irradiation, it is clear that higher oligomers must also be present. Several models of these higher oligomers and the corresponding scattering curves were tested but rejected if they led to negative ν_i or an unacceptable goodness-of-fit.

The only model that was found to give positive ν_i and acceptable values for nearly the complete set of data is the octamer shown in Figure 4. Using the basic functions for di-, tetra-, and octamers in Figure 5, it is possible to evaluate the contribution of each species to the scattering curves as a function of pH or of radiation doses as determined by the ion chamber in front of the sample. A typical fit is illustrated in Figure 6. Radiation damage results mainly in the formation of octamers at the expense of tetramers, whereas the fraction of dimers tends to increase only slightly as a function of irradiation. The calculated volume fractions, the corresponding parameters characterizing the mixtures, and the goodness-of-fit as functions of pH and irradiation time are given in Table I.

Including monomers in the fitting procedure does not give a statistically significant improvement of goodness-of-fit but leads in most cases to negative coefficients. Similar results were obtained with preparations from dried yeast.

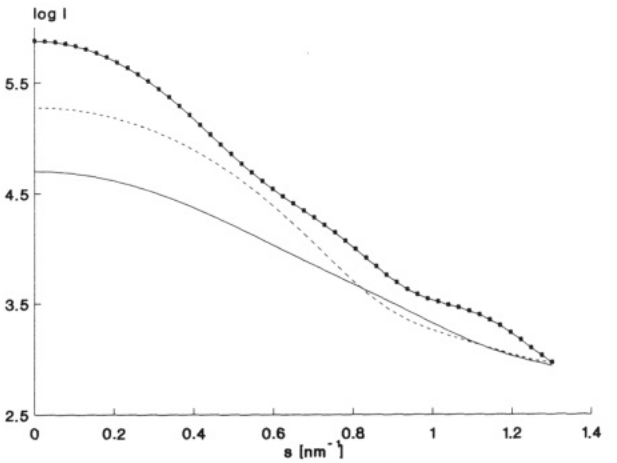

FIGURE 5: Basic scattering curves of the dimer (—), tetramer (– –), and octamer (–■–), used in the evaluation of their volume fractions. The curves have been normalized to the Porod volumes of the particles.

Figure 7 gives the volume fractions of dimers and tetramers, the only species present at low levels of irradiation, as a function of pH together with the rate of inactivation of the enzyme obtained from kinetic measurements. The latter is indirectly related to the equilibrium concentration of the catalytic species in the solution. The effect of radiation damage and the concomitant formation of octamers as a function of the absorbed dose of X-rays is shown in Figure 8.

DISCUSSION

The shape of the oligomers obtained from the analysis of the scattering curves in terms of spherical harmonics reveals interesting features of the structure of PDC in solution. The low-resolution model of the dimer [Figure 4(1,2)] corresponds closely to the assumed outline of the dimers in the tetramer [Figure 4(5)], but its maximum distance (11.1 nm) is smaller than the experimental value (13 nm). The higher resolution

Table I: Characteristics of Oligomer Mixtures as Functions of pH and Irradiation Time

pH	irrad (min)	GoF	$\langle M \rangle^a$	$\langle R_g \rangle$ (nm)	volume fractions		
					dimer	tetramer	octamer
6.2	1	0.682	4.07	3.98	−0.047 ± 0.035	1.053 ± 0.039	−0.007 ± 0.021
6.8	1	0.973	3.50	3.79	0.163 ± 0.033	0.880 ± 0.037	−0.043 ± 0.020
7.1	1	0.136	3.43	3.82	0.216 ± 0.031	0.817 ± 0.035	−0.033 ± 0.019
7.5	1	0.502	2.96	3.76	0.454 ± 0.039	0.581 ± 0.042	−0.034 ± 0.022
8.1	1	0.445	3.23	4.00	0.405 ± 0.031	0.585 ± 0.035	0.009 ± 0.018
8.4	1	0.359	1.99	3.73	0.984 ± 0.034	0.025 ± 0.036	−0.009 ± 0.018
6.8	1	0.973	3.50	3.79	0.163 ± 0.033	0.880 ± 0.037	−0.043 ± 0.020
6.8	2	0.650	3.48	3.99	0.269 ± 0.033	0.727 ± 0.037	0.004 ± 0.019
6.8	3	0.761	3.52	4.09	0.299 ± 0.032	0.671 ± 0.036	0.029 ± 0.019
6.8	4	0.455	3.43	4.13	0.363 ± 0.032	0.597 ± 0.036	0.040 ± 0.019
6.8	5	0.484	3.82	4.52	0.383 ± 0.032	0.470 ± 0.036	0.147 ± 0.019
6.8	6	0.883	3.91	4.63	0.412 ± 0.032	0.405 ± 0.035	0.183 ± 0.019
6.8	7	0.564	4.32	4.82	0.363 ± 0.032	0.375 ± 0.036	0.262 ± 0.019
6.8	8	0.053	4.58	5.01	0.405 ± 0.032	0.246 ± 0.036	0.348 ± 0.019
6.8	9	0.888	4.96	5.11	0.354 ± 0.032	0.230 ± 0.036	0.416 ± 0.019
6.8	10	0.008	5.21	5.27	0.411 ± 0.032	0.080 ± 0.036	0.509 ± 0.019

[a] Average molecular mass relative to the molecular mass of a subunit.

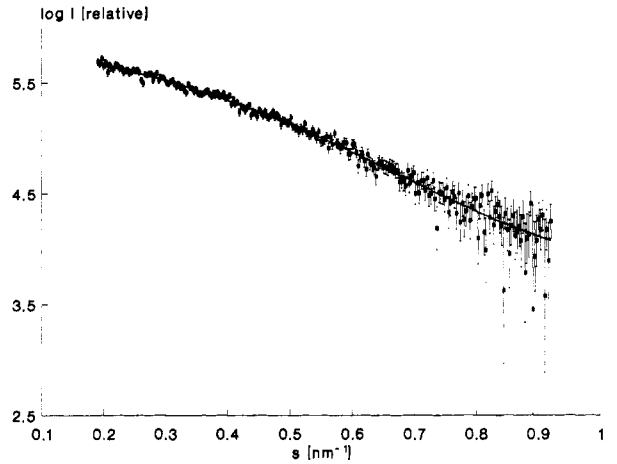

FIGURE 6: Example of a fit to the experimental data (pH 7.1, irradiation time 5 min) with the weighted sum of the basic curves shown in Figure 5. Experimental data with error bars (■); fitted curve (—); volume fractions 0.35, 0.56, 0.09; goodness-of-fit (GoF) 0.592; *z*-average R_g = 4.34 nm.

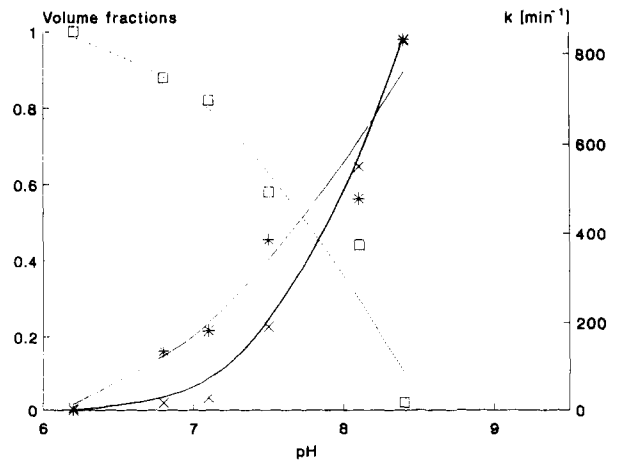

FIGURE 7: Dependence of the dimer (*) and tetramer (□) content and rate (×) of inactivation on pH. Only data corresponding to 1 min of irradiation were used in this graph.

model of the dimer in Figure 4(3) consists of two distinct subunits with dimensions of 7 × 5 × 4 nm³. This model has the correct maximum distance, but the available range of experimental data is too narrow to justify the preference of this model on a theoretical basis. In any case, the fact that the maximum distance in the tetramer does not exceed that

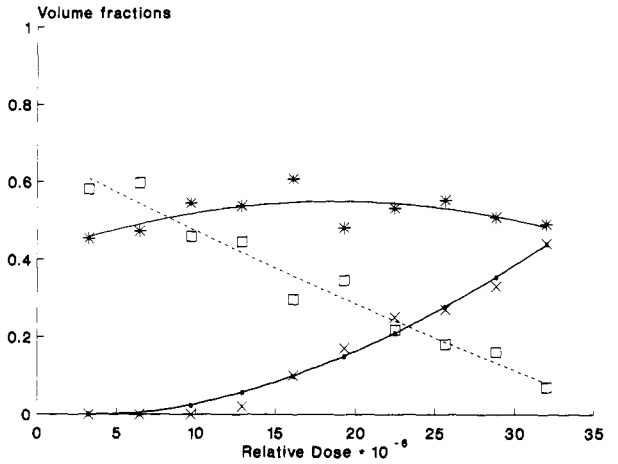

FIGURE 8: Volume fractions of dimers (*), tetramers (□), and octamers (×) as functions of the relative dose of irradiation for the sample at pH 7.5. Each interval between experimental points corresponds to 1 min of irradiation.

in the dimer implies that the dimers must undergo a conformational change when forming the tetramers, in agreement with the changes observed in the circular dichroism spectra of PDC as a function of pH (Hopmann, 1980; Ullrich & Wollmer, 1971).

The shape of the tetramer obviously results from the side-by-side association of two dimers. The latter are slightly tilted, in agreement with the electron microscopic observations of Hübner et al. (1975). Note that although no constraints were imposed in the calculations, the shapes, especially of the tetramer, clearly display the predominance of the even harmonics, as expected for the particles having an even number of nearly identical subunits. The tetramers can further associate into octamers [Figure 4(6)], but in the present study these oligomers are clearly due to radiation damage and do not exist in solutions that have not been irradiated. It can also be excluded that the solutions contain any significant amount of monomers since including monomers in the calculations of the oligomer content leads to negative values of the coefficients in eq 4.

Although the range of data is too narrow to claim that the obtained models, especially that of the dimer at L = 4, are unambiguous, the models correctly represent the general features and symmetries of the dimer as an elongated particle and of the tetramer as a globular one. A reliable evaluation

of the details of the surface requires measurements, now in progress, extending over a larger range of scattering vectors.

The main aim of the present study was the determination of the oligomer content which does not depend on the ambiguities in the detailed shapes of the dimer and the tetramer. The model of the octamer consisting of two side-by-side tetramers is the only one which allowed us to fit the complete set of data and to account for the effects of radiation damage.

Solutions of PDC in the concentration range 2–3 mg/mL thus consist of a mixture of tetramers and dimers. At pH 6.2 there are only tetramers, whereas at pH 8.4 the solution consists purely of dimers. In the range $6.8 < pH < 8.3$ there is an equilibrium between dimers and tetramers which is only displaced toward tetramers or dimers at the ends of the range. These results were recently confirmed by ultracentrifugation (Hübner, König, and Schellenberg, unpublished data). Since Van Urk et al. (1989) have measured the pH of yeast cytosol and obtained values of 6.8–6.9, this suggests that an equilibrium between dimers and tetramers also exists in the cell.

Previous studies have shown that the cofactors of PDC (thiamin diphosphate and Mg^{2+}) are released at pH 7 and that at pH 8.5 a catalytically totally inactive apoenzyme is obtained (Schellenberger & Hübner, 1967). The optimal enzymatic activity is obtained at pH 6 and the maximum stability at pH 5.5. Taking the structural and kinetic data together, it can thus be unequivocally concluded that only the tetramers of PDC are catalytically active, also in physiological conditions. In the cytosol, an accumulation of the substrate pyruvate should result in a reduction of the pH, thereby displacing the equilibrium toward tetramers. This suggests that the pH-dependent equilibrium between oligomers could be, besides substrate activation, a further regulation mechanism of PDC at the molecular level.

The present analysis was made possible by the high brilliance of synchrotron radiation sources which allows one to record statistically significant data in considerably shorter times than on conventional sources and thus to monitor radiation damage. This is encouraging for measurements on the next generation of storage rings, where considerably more brilliant sources can be expected in the near future. The methods described here can be readily extended to time-resolved measurements using stroboscopic methods, but each experimental run will then have to be analyzed and compared with the previous one before averaging.

ACKNOWLEDGMENT

We thank Mrs. Brauer for her expert assistance in the preparation of PDC.

REFERENCES

Bevington, P. R. (1969) *Data reduction and error analysis for the physical sciences*, McGraw-Hill, New York.

Boulin, C., Kempf, R., Koch, M. H. J., & McLaughlin, S. M. (1986) *Nucl. Instrum. Methods Phys. Res. A249*, 399–407.

Boulin, C., Kempf, R., Gabriel, A., & Koch, M. H. J. (1988) *Nucl. Instrum. Methods Phys. Res. A269*, 312–320.

Bringer-Meyer, S., Schimz, K. L., & Sahm, H. (1986) *Arch. Microbiol. 146*, 105–110.

Dyda, F., Furey, W., Swaminathan, S., Sax, M., Farrenkopf, B., & Jordan, F. (1990) *J. Biol. Chem. 265*, 17413–17415.

Feigin, L. A., & Svergun, D. I. (1987) *Structure Analysis by Small-Angle X-ray and Neutron Scattering*, Plenum Press, New York.

Gounaris, A. D., Turkenkopf, I., & Greenlie, J. (1975) *Biochim. Biophys. Acta 405*, 492–499.

Gubler, R., & Wittorf, J. H. (1970) *Methods Enzymol. 18*, 117–120.

Hohmann, S., & Cederberg, H. (1990) *Eur. J. Biochem. 188*, 615–621.

Holzer, H., Schultz, G., Villar-Palasi, C., & Jüntgen-Sell, J. (1956) *Biochem. Z. 327*, 331–344.

Hopmann, R. F. W. (1980) *Eur. J. Biochem. 110*, 311–318.

Hübner, G., Schellenberger, A., Stelmaschuk, V. Y., & Kiselev, N. A. (1975) *Acta Biol. Med. Ger. 34*, 699–701.

Hübner, G., König, S., Schellenberger, A., & Koch, M. H. J. (1990) *FEBS Lett. 266*, 17–20.

Jordan, F., Farzani, K., & Akinyosoyl, P. (1979) *Jerusalem Symp. Quant. Chem. Biochem. 12*, 131–146.

Koch, M. H. J. (1991) in *Handbook on Synchrotron Radiation* (Ebashi, S., Koch, M., & Rubenstein, E., Eds.) Vol. 4, pp 241–264, Elsevier Science Publishers, Amsterdam.

Koch, M. H. J., & Bordas, J. (1983) *Nucl. Instrum. Methods 208*, 461–469.

Koike, K., & Koike, M. (1982) *Bitamin 56*, 665–673.

Kuo, D. J., Pikdan, G., & Jordan, F. (1986) *J. Biol. Chem. 261*, 3316–3319.

Leblova, S., & Martinec, J. (1987) *Biologia (Bratislava), 42*, 1181–1189.

Leblova, S., & Valik, J. (1981) *Biol. Plant 23*, 81–85.

Leblova, S., Malik, M., & Fojta, M. (1989) *Biologia (Bratislava), 44*, 329–383.

Lee, T. C., & Langston-Unkefer, P. J. (1985) *Plant Physiol. 79*, 242–247.

Müller, J. J., Damaschun, G., & Hübner, G. (1979) *Acta Biol. Med. Ger. 38*, 1–10.

Neale, A. D., Scopes, R. K., Wettenhall, R. E. H., & Hoogenraad, N. J. (1987) *J. Bacteriol. 169*, 1024–1028.

Neuberg, C., & Karczag, L. (1911) *Biochem. Z. 36*, 68–75.

Oba, K., & Uritani, I. (1975) *J. Biochem. 77*, 1205–1213.

Pilz, I., & Ullrich, J. (1973) *Eur. J. Biochem. 34*, 256–261.

Sanemori, H., Yoshida, S., & Kawasaki, T. (1974) *J. Biochem. 75*, 123–129.

Schellenberger, A. (1982) *Ann. N. Y. Acad. Sci. 387*, 51–62.

Schellenberger, A., & Hübner, G. (1967) *Hoppe-Seyler's Z. Physiol. Chem. 348*, 491–500.

Sieber, M., König, S., Hübner, G., & Schellenberger, A. (1983) *Biomed. Biochim. Acta 42*, 343–349.

Stuhrmann, H. B. (1970a) *Acta Crystallogr. A26*, 297–306.

Stuhrmann, H. B. (1970b) *Z. Phys. Chem. (Frankfurt) 72*, 177–184, 185–198.

Svergun, D. I. (1991) *J. Appl. Crystallogr. 24*, 485–492.

Svergun, D. I., & Stuhrmann, H. B. (1991) *Acta Crystallogr. A47*, 736–744.

Svergun, D. I., Semenyuk, A. V., & Feigin, L. A. (1988) *Acta Crystallogr. A44*, 244–250.

Ullrich, J., & Kempfle, M. (1969) *FEBS Lett. 4*, 273–274.

Ullrich, J., & Wollmer, A. (1971) *Hoppe-Seyler's Z. Physiol. Chem. 352*, 1635–1644.

Ullrich, J., Wittorf, J. H., & Gubler, C. J. (1966) *Biochim. Biophys. Acta 113*, 595–604.

Van Urk, H., Schipper, D., Breedveld, G. J., Mak, P. R., Scheffers, W. A., & Van Dijken, J. P. (1989) *Biochim. Biophys. Acta 992*, 78–86.

Zehender, H., & Ullrich, J. (1985) *FEBS Lett. 180*, 51–54.

Zehender, H., Trescher, D., & Ullrich, J. (1987) *Eur. J. Biochem. 167*, 149–154.

Zeng, X., Chung, A., Haran, M., & Jordan, F. (1991) *J. Am. Chem. Soc. 113*, 5842–5849.

Registry No. PDC, 9001-04-1.